Protein Science (1992), *1*, 310-321. Cambridge University Press. Printed in the USA.

NMR structure of oxidized *Escherichia coli* glutaredoxin: Comparison with reduced *E. coli* glutaredoxin and functionally related proteins

TAI-HE XIA,[1] JOHN H. BUSHWELLER,[1] PATRICK SODANO,[1] MARTIN BILLETER,[1] OLOF BJÖRNBERG,[2] ARNE HOLMGREN,[2] AND KURT WÜTHRICH[1]

[1] Institut für Molekularbiologie und Biophysik, Eidgenössische Technische Hochschule-Hönggerberg, CH-8093 Zürich, Switzerland

[2] Department of Biochemistry, Karolinska Institute, S-10401 Stockholm, Sweden

(RECEIVED October 21, 1991; ACCEPTED November 7, 1991)

Abstract

The determination of the NMR structure of oxidized *Escherichia coli* glutaredoxin in aqueous solution is described, and comparisons of this structure with that of reduced *E. coli* glutaredoxin and the related proteins *E. coli* thioredoxin and T4 glutaredoxin are presented. Based on nearly complete sequence-specific ^{1}H-NMR assignments, 804 nuclear Overhauser enhancement distance constraints and 74 dihedral angle constraints were obtained as the input for the structure calculations, for which the distance geometry program DIANA was used followed by simulated annealing with the program X-PLOR. The molecular architecture of oxidized glutaredoxin is made up of three helices and a four-stranded β-sheet. The three-dimensional structures of oxidized and the recently described reduced glutaredoxin are very similar. Quantitative analysis of the exchange rates of 34 slowly exchanging amide protons from corresponding series of two-dimensional [^{15}N,^{1}H]-correlated spectra of oxidized and reduced glutaredoxin showed close agreement, indicating almost identical hydrogen-bonding patterns. Nonetheless, differences in local dynamics involving residues near the active site and the C-terminal α-helix were clearly manifested. Comparison of the structure of *E. coli* glutaredoxin with those of T4 glutaredoxin and *E. coli* thioredoxin showed that all three proteins have a similar overall polypeptide fold. An area of the protein surface at the active site containing Arg 8, Cys 11, Pro 12, Tyr 13, Ile 38, Thr 58, Val 59, Pro 60, Gly 71, Tyr 72, and Thr 73 is proposed as a possible site for interaction with other proteins, in particular ribonucleotide reductase. It was found that this area corresponds to previously proposed interaction sites in T4 glutaredoxin and *E. coli* thioredoxin. The solvent-accessible surface area at the active site of *E. coli* glutaredoxin showed a general trend to increase upon reduction. Only the sulfhydryl group of Cys 11 is exposed to the solvent, whereas that of Cys 14 is buried and solvent inaccessible.

Keywords: glutaredoxin; NMR; protein structure; redox enzymes; thioredoxin

Glutaredoxin from *Escherichia coli* is a small protein (85 residues, $M_r \approx 10{,}000$) involved in electron transfer reactions via the reversible oxidation of two SH groups to a disulfide bond (Holmgren, 1989). In the oxidized form, its active site is formed by a 14-membered loop consisting of the sequence

Cys 11–Pro 12–Tyr 13–Cys 14

closed by a disulfide bridge between the two cysteines (Höög et al., 1983). *Escherichia coli* glutaredoxin, which catalyzes glutathione-dependent redox reactions such as reduction of ribonucleotides with ribonucleotide reductase, belongs to a family of functionally related proteins (Holmgren, 1985). For several members of this family three-dimensional (3D) structures have been reported. The solution structure of the oxidized *E. coli* glutaredoxin is presented here; the structure of its reduced form was described earlier (Sodano et al., 1991b). The NMR structure of the reduced form of *E. coli* thioredoxin, a related protein, was recently presented by Dyson et al. (1990); the

Reprint requests to: K. Wüthrich, Institut für Molekularbiologie und Biophysik, Eidgenössische Technische Hochschule-Hönggerberg, CH-8093 Zürich, Switzerland.

structure of the oxidized form of this protein was determined by X-ray crystallography (Holmgren et al., 1975; Katti et al., 1990). The crystal structure of glutaredoxin from the phage T4 is also known (Söderberg et al., 1978; Eklund et al., 1992; this protein was formerly known as T4 thioredoxin). In addition, the sequences of three mammalian glutaredoxins have now been determined (Hopper et al., 1989).

In an earlier publication we described NMR experiments, sequence-specific ^{1}H-NMR assignments, and the identification of regular secondary structures in the oxidized form of *E. coli* glutaredoxin (Sodano et al., 1991a). Here, we present the complete 3D solution structure of this protein determined by NMR and distance geometry and compare it to the structure obtained for the reduced form (Sodano et al., 1991b). Furthermore, the structures of oxidized and reduced *E. coli* glutaredoxin are compared with the crystal structure of phage T4 glutaredoxin (Eklund et al., 1992) and the two known structures of *E. coli* thioredoxin (Dyson et al., 1990; Katti et al., 1990).

Table 1. *Summary of input constraints used for the determination of the structure of the oxidized form of E. coli glutaredoxin, and of residual violations of the conformational constraints*

		Residual violations	
Constraints	n	n^a	Sum[b]
Intraresidual NOEs	241	1.3	1.4-2.6 Å
Sequential NOEs	181	0.6	0.1-1.3 Å
Medium-range NOEs	163	0.8	0.6-1.9 Å
Long-range NOEs	219	0.2	0.6-1.5 Å
Total NOEs	804	2.8	3.3-6.2 Å
ϕ angle constraints	56	0.2	0.5-20.6°
χ^1 angle constraints	18	0.2	0.0-12.3°

[a] The number of residual violations exceeding the following thresholds, averaged over the 20 individual conformers, is given: NOE distance constraints > 0.2 Å; dihedral angle constraints > 5°.

[b] The ranges for the 20 conformers of the sums of residual violations are reported.

Results

Sequence-specific resonance assignments for 95% of the backbone protons in oxidized glutaredoxin have been described earlier (Sodano et al., 1991a). One or two β-protons were assigned for all but three nonglycine residues; more peripheral protons for all but six of the side chains containing such protons. These data provided the basis for the presently described determination of the 3D structure.

Determination of the structure of the oxidized form of E. coli glutaredoxin

Table 1 summarizes the experimental NMR data used as input for the structure calculation. Of the 804 nuclear Overhauser enhancement (NOE) distance constraints used, 219 have a sequence range exceeding five residues. The distribution of these long-range constraints is very similar to the one obtained for the reduced glutaredoxin (Sodano et al., 1991b), i.e., only a few long-range constraints were observed for residues 8-14, 26-30, and 39-47. In all, 62 coupling constants of the type $J_{HN\alpha}$ and 36 couplings of the type $J_{\alpha\beta}$ could be measured, yielding a constraint for a ϕ angle or a χ^1 angle, respectively. Seven of the 18 constraints on χ^1 angles affect aromatic residues. The initial analysis of the coupling constants $J_{HN\alpha}$ and $J_{\alpha\beta}$ and the intraresidual and sequential backbone-backbone NOEs with the program HABAS (Güntert et al., 1989), together with inspection of the structures obtained in a first round of distance geometry calculations with the program GLOMSA (Güntert et al., 1991b) allowed the establishment of individual assignments for 25 pairs of diastereotopic substituents and side-chain amide protons (Table 2). The calculation of the solution structure of the oxidized form of *E. coli* glutaredoxin with the programs DIANA (Güntert et al., 1991a) and X-PLOR (Brünger, 1990) followed exactly the procedure described for the reduced form of glutaredoxin (Sodano et al., 1991b).

The structure of the oxidized form of E. coli glutaredoxin

Figure 1 shows a superposition of the 20 final conformers of oxidized *E. coli* glutaredoxin obtained by distance geometry and simulated annealing. The structure consists of a four-stranded β-sheet with residues 2-7, 32-37, 61-64, and 67-69, and three helices with residues 15-28, 45-53, and 71-83 (Fig. 2; Kinemages 1, 2). The outer strand 32-37 runs parallel to the strand 2-7, and the strand 61-64 is antiparallel to both 2-7 and 67-69. The axes of the helices 15-28 and 71-83 are parallel to the β-strands, and their direction is opposite to the direction of the first β-strand. The position and the orientation of the second helix is not well determined. The residual violations of the input constraints are summarized in Table 1. Practically all violations are smaller than 0.2 Å for distance constraints and smaller than 5° for dihedral angle constraints. The final energies calculated with the program X-PLOR (Brünger, 1990) range from −1,486 to −1,649 kcal/mol. All bond lengths differ from their ideal value by less than 0.05 Å, with a root mean square distance (r.m.s.d.) of 0.007 Å. The corresponding two numbers for bond angles are 8.5° and 1.9°. The r.m.s.d. values from the 20 individual conformers to their averaged coordinates for various selections of heavy atoms are

Table 2. *Chemical shifts of residues with individually assigned diastereotopic substituents and side-chain amide protons in oxidized E. coli glutaredoxin in aqueous solution at pH 7.0 and 28 °C*[a]

	Chemical shift δ (ppm)[b]			
Residue	NH	αH	βH	Others
Val 4	9.38	4.69	1.70	γCH_3 *0.17, 0.64*
Val 15	7.42	3.54	2.16	γCH_3 *0.91, 1.04*
Lys 18	8.00	3.59	*1.71, 1.92*	γCH_2 1.49; δCH_2 1.23, 1.02; ϵCH_2 2.72
Leu 20	7.80	4.28	*1.82, 2.14*	γH 1.35; δCH_3 *0.89, 0.61*
Lys 23	7.80	4.05	*1.90, 2.04*	
Leu 24	8.02	3.77	*1.12, 0.00*	γH 1.50; δCH_3 *0.35, 0.52*
Asp 30	8.37	4.69	*3.09, 2.59*	
Phe 31	8.06	4.93	*2.69, 3.26*	δH 7.26, 7.26; εH 7.43, 7.43; ζH 7.26
Gln 32	7.97	4.96	*1.95, 2.13*	γCH_2 2.39, 2.28; ϵNH_2 7.51, 6.99
Val 36	8.71	3.87	1.39	γCH_3 *0.70, 0.30*
Ile 38	9.23	3.87	2.50	γCH_2 *1.36, 1.57*; γCH_3 1.15; δCH_3 0.76
Glu 41	7.82	4.40	*1.60, 2.26*	γCH_2 2.35
Leu 48	7.74	3.64	*1.75, 1.12*	γH 1.41; δCH_3 *0.51, 0.06*
Phe 63	9.04	5.22	*2.95, 2.57*	δH 7.22, 7.22; εH 6.80, 6.80; ζH 7.19
Val 64	8.67	4.48	1.26	γCH_3 *0.65, 0.27*
His 68	9.18	3.57	*2.86, 3.00*	δ^2H 5.55; ϵ^1H 7.52
Ile 69	8.23	3.87	1.34	γCH_2 *1.14, 0.49*; γCH_3 0.51; δCH_3 −0.12
Tyr 72		3.99	*3.26, 2.82*	δH 6.79, 6.79; εH 6.69, 6.69
Trp 78	8.26	4.02	*3.33, 3.62*	δ^1H 7.27; ϵ^3H 7.38; ϵ^1NH 10.18; ζ^2H 7.41; ζ^3H 6.99; η^2H 7.37
Val 79	8.80	3.16	1.92	γCH_3 *0.75, 0.62*
Asn 82	7.72	4.47	1.79, 1.07	δNH_2 *6.02, 6.89*
Leu 83	7.91	4.48	1.68, 1.43	γH 1.28; δCH_3 *0.91, 0.77*

[a] The experimental conditions were the same as for the previously reported sequence-specific resonance assignments (Sodano et al., 1991a).

[b] The chemical shift values for the individually assigned diastereotopic substituents and side-chain amide protons are printed in italics and underlined, and the first value is the shift of the proton or methyl group with the lower branch number, e.g., the β^2 proton, or the γ^1 methyl group in Val.

Fig. 1. Stereo view of the 20 conformers of the oxidized form of *E. coli* glutaredoxin used to characterize the solution conformation. The structures were superimposed by fitting N, C^{α}, and C′ of residues 1–8, 13–43, and 60–83 of the conformers 2–20 for minimal r.m.s.d. relative to conformer 1 (which has the smallest residual violations). For each conformer all bonds connecting N, C^{α}, and C′ are shown.

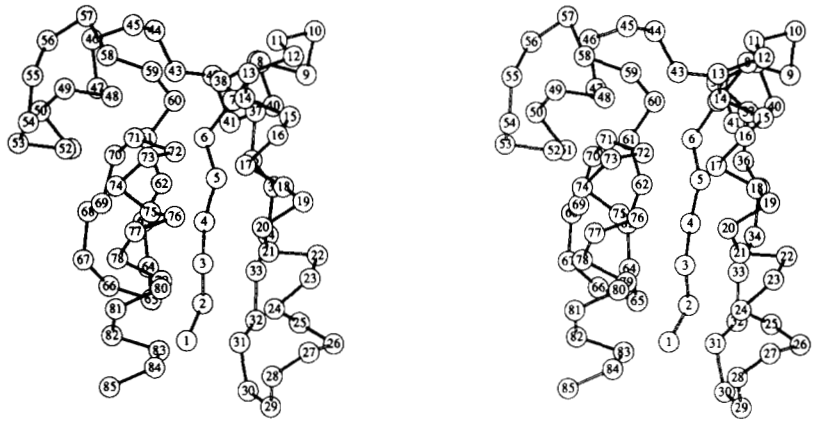

Fig. 2. Stereo view of a ball-and-stick model of the conformer of *E. coli* glutaredoxin from Figure 1, which has the lowest r.m.s.d. relative to the mean coordinates.

Table 3. *Root mean square deviation values among the 20 conformers of oxidized, as well as reduced, E. coli glutaredoxin (Fig. 1) calculated for four different selections of atoms*[a]

Atoms used for the comparison	⟨OX⟩-OX[b] (Å)	⟨RED⟩-RED[b] (Å)	⟨OX⟩-⟨RED⟩[b] (Å)
N, C^{α}, C′ of 1–85	1.1 ± 0.1	1.0 ± 0.1	1.05
N, C^{α}, C′ of 1–8, 13–43, 60–83	0.8 ± 0.1	0.7 ± 0.1	0.72
Same plus core side chains[c]	0.7 ± 0.1	0.7 ± 0.1	0.72
N, C^{α}, C′ of 11–14	0.3 ± 0.1	0.5 ± 0.1	0.74

[a] For comparison, r.m.s.d. values are also presented for the reduced form of the protein, and the mean structures of the two species are compared.

[b] ⟨OX⟩ and ⟨RED⟩ denote, respectively, the averaged coordinates of the 20 conformers that represent the solution structures of the oxidized and reduced forms of *E. coli* glutaredoxin. OX and RED represent the set of 20 conformers of the oxidized and reduced form, respectively.

[c] The core side chains are those of the following 27 residues: 3–6, 15, 17, 20, 21, 24, 25, 31, 33, 35, 36, 38, 62–64, 68, 69, 72, 75–79, 83 (residues 17, 21, 76, and 77 are alanines).

reported in Table 3 (first column). For the N, C^{α}, and C′ atoms of the complete polypeptide backbone, a value of 1.1 Å was obtained. This value is reduced to 0.8 Å when only the backbone atoms of residues 1–8, 13–43, and 60-83 are considered, which corresponds to about 75% of the total chain length.

Apparent structural disorder, indicated by a large dispersion among the 20 conformers in Figure 1 (Wüthrich, 1986, 1989), is found for the residues 44–59, which include the second helix. The helix as such is, however, well characterized as a regular secondary structure. This is demonstrated in Figures 3 and 4. The solid line in Figure 3 represents the local r.m.s.d. values calculated for the backbone superposition of tripeptides and plotted for the central residue. With the exception of the second helix (residues 45–53), the residues 9–12, 44–59, and 84–85, which have not been included among the well-defined parts of the structure in the global fits of Figure 1 and Table 3, are also part of locally disordered regions, with values of r.m.s.d.(3) >0.3 Å in Figure 3. The heavy lines and circles in Figure 4 show the structural variations for the C^{α} atoms of the individual residues in oxidized glutaredoxin after global superposition for minimal r.m.s.d. of the backbone atoms of residues 1–8, 13–43, and 60–83. The circles indicate the average displacement of the C^{α} atoms from the mean coordinates given by the heavy line. It shows that the second helix experiences large structural variance within the set of 20 conformers, in spite of the low local r.m.s.d. values (Fig. 3).

All residues for which the normalized structural variation of the side-chain heavy atoms after global superposition for minimal r.m.s.d. of the backbone atoms of residues 1–8, 13–43, and 60–83 of the 20 final conformers was smaller than 1.4 Å were selected as best-defined core side chains (see the footnote to Table 3 for a list of these 27 residues). Inclusion of these side chains into the calculation of the r.m.s.d. does not increase the r.m.s.d. value over the one calculated for the backbone atoms

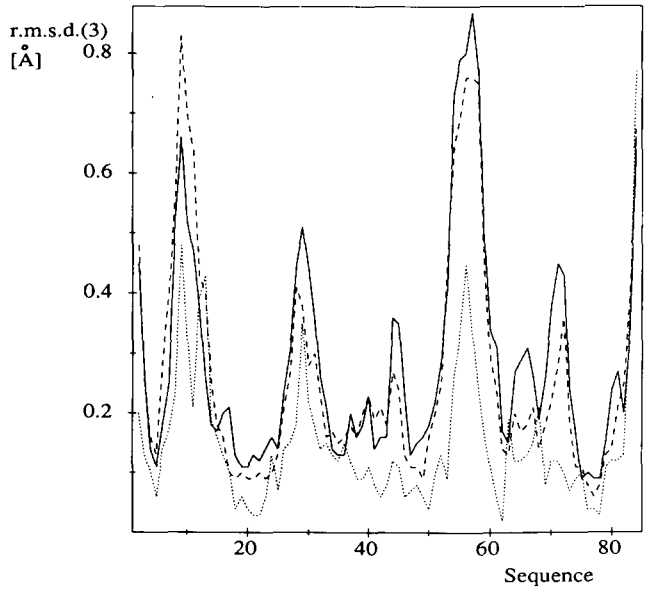

Fig. 3. Local r.m.s.d. values for the backbone superposition of all tripeptides along the sequence are plotted at the positions of the central residues. Solid line: averaged values of the 190 pairwise comparisons among the 20 individual NMR conformers of the oxidized form of *E. coli* glutaredoxin. Dashed line: same for the reduced protein. The dotted line represents the local r.m.s.d. between the averaged coordinates of the oxidized and the reduced form.

alone (Table 3). These side chains, which include 20 hydrophobic residues, are mostly located in the interior of the protein, thus stabilizing the spatial arrangement of the regular secondary structures of the protein.

Comparison of the NMR structures obtained for oxidized and reduced E. coli glutaredoxin

The comparison of the oxidized and reduced forms of *E. coli* glutaredoxin reveals a strong similarity between the two structures, and the quality of the structure determination is also very similar for the two forms. The local r.m.s.d. values for tripeptides for the oxidized form (solid line in Fig. 3) follows closely the corresponding line for the reduced form (dashed line), and the local differences between the averaged coordinates of the two forms (dotted line in Fig. 3) are nearly always smaller than the r.m.s.d.'s for the groups of conformers representing the individual proteins. The two proteins thus clearly contain nearly identical secondary structures. In general, the local structure of the reduced form is slightly better determined, except that due to the formation of the disulfide bridge between Cys 11 and Cys 14, the polypeptide backbone in the active site is better defined in the oxidized form, as documented by the r.m.s.d. values for this segment of 0.3 Å for the oxidized form and 0.5 Å for the reduced form (Table 3).

The global coincidence between the structures of the two forms of glutaredoxin is shown in Figure 4. The circles in this figure indicate the spread of the backbone atoms after superposition for best fit of N, C^{α}, and C′ of the segments 1–8, 13–43, and 60–83. The backbone line of each structure passes through the circles defining the uncertainty in the determination of the other structure, showing that the two structures coincide within the precision of the experiments. The structural variability in the oxidized form is slightly larger than in the reduced form,

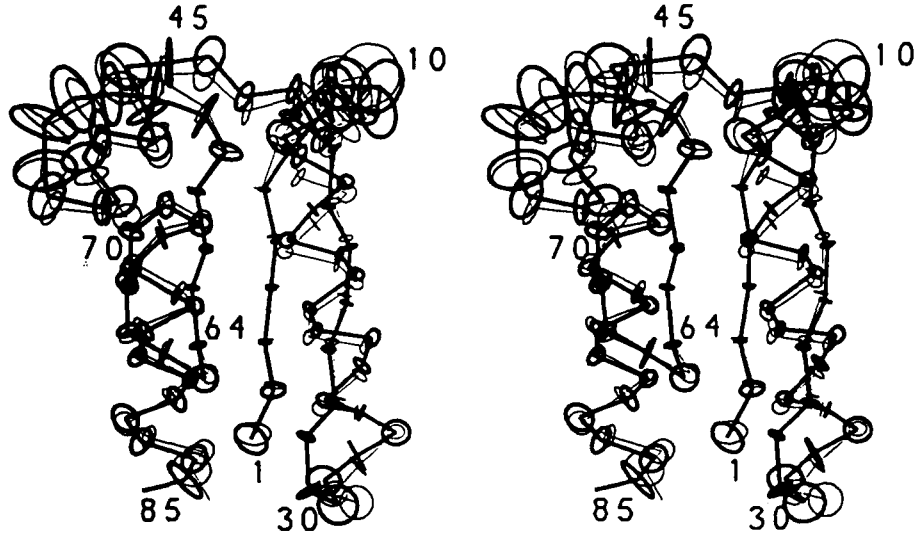

Fig. 4. Superposition obtained by a global fit of N, C^{α}, and C′ of residues 1–8, 13–43, and 60–83 of the averaged coordinates of the 20 conformers representing the oxidized (heavy line) and the reduced (thin line) form of *E. coli* glutaredoxin, respectively. In this stereo view, the polypeptide backbone is represented by virtual bonds connecting successive C^{α} atoms, and the orientation is the same as in Figure 1. The circles around the C^{α} positions indicate the variation of the 20 individual NMR conformers after superposition for minimal r.m.s.d. with the averaged coordinates.

in particular near the ends of regular secondary structure elements. The agreement of the two structures extends to the well-defined core side chains (Table 3), which essentially describe a hydrophobic cluster in the interior of the protein. Table 3 quantifies the above observations in terms of r.m.s.d. values. Except for the comparison of the active site, the corresponding r.m.s.d. values within each group of 20 conformers are very similar, and almost the same values are found again between the averaged coordinates of the two forms.

Comparison of amide proton exchange rates of oxidized and reduced glutaredoxin

Because the structures of oxidized and reduced glutaredoxin are so similar, we wished to compare the amide exchange rates for the two forms of the protein to see if there were any significant differences indicative of altered dynamics between the two forms. Because the exchange data were originally collected in different ways for oxidized and reduced glutaredoxin (Sodano et al., 1991a,b), we chose to collect new data in a uniform manner for both, namely to observe the exchange of the amide protons in [^{15}N–^{1}H] 2D-correlated spectroscopy (COSY) spectra (Bodenhausen & Ruben, 1980) recorded in freshly prepared D_2O solutions of the ^{15}N-labeled protein. A total of 34 slowly exchanging amide protons were identified (Table 4) as described in the Methods section. The same 34 protons were found to exchange slowly in both the oxidized and reduced proteins, indicating again the close similarity of the two forms. Of the 34 slowly exchanging amide protons identified in this manner, 30 and 29, respectively, were identified as being consistently hydrogen-bonded in the calculated structures of reduced and oxidized glutaredoxin (see Table 4). In order to examine the exchange data more quantitatively, rates of exchange were calculated for all those amide protons for which the resonances were well separated in the heteronuclear COSY

Table 4. *Comparison of hydrogen bonds involving backbone atoms and of amide proton exchange rates in the solution structures of oxidized and reduced E. coli glutaredoxin*

				k_{ex} (10^{-3} min^{-1})[b]						k_{ex} (10^{-3} min^{-1})	
Donor NH	Acceptor O	OX[a]	RED[a]	OxGrxEC	RedGrxEC	Donor NH	Acceptor O	OX	RED	OxGrxEC	RedGrxEC
Thr 3	Gln 32	18	18	5.3	5.3	Glu 41	Asp 37	16			
Val 4	Phe 63	20	20	1.1	1.4	Gly 42	Ile 38	15	10		
Ile 5	Gln 34	16	20	1.5	0.79	Ile 43	Ile 38	20	20		
Phe 6	Gln 61	19	20	0.64	1.2	Leu 48	Thr 44		12		
Gly 7	Val 36	18	14	1.5	2.8	Gln 49	Lys 45	13	19		
Val 15	Cys 11	14				Gln 50	Glu 46	12	20		
Arg 16	Pro 12	12				Lys 51	Asp 47	15	13		
Arg 16	Tyr 13		12			Ala 52	Leu 48	12	18		
Ala 17				2.3	6.3	Gly 53	Gln 49	15	18		
Lys 18	Cys 14		17	o	3.0	Gln 61	Phe 6		17	2.0	2.0
Asp 19	Val 15	18	19	1.4	1.8	Ile 62	Gly 70	12	18	1.3	0.73
Leu 20	Arg 16	13	20	1.8	1.2	Phe 63	Val 4	20	20	o	o
Ala 21	Ala 17	16	20	1.5	1.1	Val 64	Gln 67	16	20	o	o
Glu 22	Lys 18	18	20	1.5	1.2	Asp 65	Gln 2	14	18		
Lys 23	Asp 19	18	20	2.2	2.3	Gln 67	Val 64	14	18	10	6.5
Leu 24	Leu 20	17	18	o	o	Ile 69	Ile 62	19	20	2.6	4.1
Ser 25	Ala 21	18	20	2.8	3.1	Gly 70				3.9	7.0
Asn 26	Gln 22		16		6.5	Phe 75	Gly 71	12	15	4.3	5.7
Asn 26	Lys 23	14		7.5		Ala 76	Tyr 72	19	17	o	o
Glu 27	Lys 23	11				Ala 77	Thr 73	18	16	11	5.0
Glu 27	Leu 24		10			Trp 78	Asp 74	20	18	1.8	0.71
Arg 28	Leu 24	17	17	o	o	Val 79	Phe 75	20	20	0.77	0.29
Gln 32	Met 1	18	14	2.5	1.6	Lys 80	Ala 76	16	18	15	8.6
Gln 34	Thr 3	20	18	1.4	1.5	Glu 81	Ala 77	15			
Tyr 35				o	o	Asn 82	Trp 78	12			
Val 36	Ile 5	18	20	1.5	0.60	Asn 82	Val 79		11		
Ile 38	Gly 7	15		6.3	4.8	Leu 83	Val 79	17	18		
Ala 40	Asp 37	14				Asp 84	Lys 80	11			

[a] OX and RED stand for the group of 20 conformers used to represent the solution structures of oxidized and reduced glutaredoxin, respectively. In these columns those hydrogen bonds that were identified in 10 or more of the 20 conformers are listed, otherwise no number is given.

[b] OxGrxEC and RedGrxEC stand for oxidized and reduced glutaredoxin from *E. coli*, respectively. In these columns, o indicates that the respective amide proton was identified as having slowed exchange, but a quantitative evaluation of the exchange rate was not possible because of spectral overlap.

```
GrxEC  QTVIFGR ... CPYCVRAKDLAEKLS ... YQYVDIR ... PQIFV ... QHIGGYTDFAAWVK
         2      8    11              25   33      39   60   64   67      72      80
GrxT4  MFKVYGY ... CVYCDNAKRLLTVKK ... FEFINIM ... PQVFA ... SHIGGFDQLREYFK
         1      7    14              28   31      37   66   70   74      79      87
TrxEC  ILVDFWA ... CGPCKMIAPILDEIA ... VAKLNID ... PTLLL ... ATKVGA
        23     29   32              46   55      61   76   80   88      93
```

Fig. 5. Sequence alignments of *E. coli* glutaredoxin (GrxEC), T4 glutaredoxin (GrxT4), and *E. coli* thioredoxin (TrxEC). Below each sequence the residue numbering for the protein is given. This alignment includes only residues that could be unambiguously aligned on the basis of the 3D structures. Relative to the alignment proposed by Eklund et al. (1991) the underlined residues of *E. coli* glutaredoxin are shifted by one position to the left for residues 2–8, respectively, and to the right for residues 72–80.

spectra. Overall, the exchange rates for corresponding residues in the two forms of the protein agree quite closely (Table 4), but there are limited regions that are consistently different in the two states. In particular, several residues neighboring the active site, i.e., Phe 6, Gly 7, and Ala 17, show an enhanced rate of exchange in the reduced protein, suggestive of greater flexibility in this region upon cleavage of the disulfide bond. The residues Gln 67, Ile 69, and Gly 70 of the fourth β-strand also show differences between the two states. These residues precede a polypeptide segment, 71–73, which may play a role in the protein–protein interactions of glutaredoxin (see below), so that the difference in the local dynamics observed here is quite interesting. Finally, the rates of exchange for residues identified in the C-terminal helix are slower in the reduced form than in the oxidized form. Interestingly, the results of the structure calculations (Table 4) show a difference in the hydrogen-bonding pattern for the final residues of this helix. There does appear, therefore, to be some change in the dynamics of the last helix upon reduction, but the manner in which the change is transmitted from the active-site region is not readily discernible in the structures (Fig. 1).

Discussion

The biological importance of *E. coli* glutaredoxin, particularly as a reductant for ribonucleotide reductase, warrants comparison with proteins of similar function as well as a careful examination of the active-site region to better understand the functional importance of residues in this region.

Comparisons of various glutaredoxins and thioredoxins

A number of other proteins involved in electron transfer reactions have been studied, and the atomic structures are known for *E. coli* thioredoxin (NMR solution structure of the reduced form by Dyson et al. [1990]; high-resolution X-ray crystal structure of the oxidized form by Katti et al. [1990]) and for oxidized glutaredoxin from the T4 phage (X-ray crystal structure by Eklund et al. [1991]). The alignment of 40 residues for the three different proteins in Figure 5 is proposed on the basis of the superposition of the corresponding 3D structures. Residues 2–8, 33–39, 60–64, and 67–72 of *E. coli* glutaredoxin, which include the complete four-stranded β-sheet, correspond to residues 1–7, 31–37, 66–70, and 74–79 in T4 glutaredoxin, and to residues 23–29, 55–61, 76–80, and 88–93 of *E. coli* thioredoxin. Residues 11–25 in *E. coli* glutaredoxin, i.e., the active site and the first helix, correspond to residues 14–28 in T4 glutaredoxin and to residues 32–46 in *E. coli* thioredoxin. For the residues 2–8 and 72–80 of *E. coli* glutaredoxin this alignment differs by one residue position from the one given by Eklund et al. (1992). Table 5 gives the r.m.s.d. comparisons for the 40 residues aligned in Figure 5. The glutaredoxins from *E. coli* and phage T4 resemble each other to a higher extent

Table 5. *Root mean square deviation comparisons between the solution structures of the oxidized and reduced forms of E. coli glutaredoxin and reduced E. coli thioredoxin, and the crystal structures of oxidized E. coli thioredoxin and T4 glutaredoxin*[a]

	⟨RED⟩	OxGrxT4	OxTrxEC	RedTrxEC
⟨OX⟩	0.7	0.9	1.4	1.4
⟨RED⟩		1.0	1.6	1.5
OxGrxT4			1.3	1.3
OxTrxEC				0.6

[a] The different structures are identified by the following symbols: ⟨OX⟩ and ⟨RED⟩ define the averaged coordinates of the 20 NMR conformers of the oxidized and the reduced forms of *E. coli* glutaredoxin, OxGrxT4 is the crystal structure of oxidized glutaredoxin from T4 phage (Eklund et al., 1992), OxTrxEC is the single crystal structure of the oxidized thioredoxin from *E. coli* (Katti et al., 1990), and RedTrxEC represents the averaged coordinates of 12 NMR conformers of the reduced thioredoxin from *E. coli* (Dyson et al., 1990). Forty residues were used to calculate the r.m.s.d. values for the backbone atoms N, C^{α}, and C′ presented in this table, namely residues 2–8, 11–25, 33–39, 60–64, and 67–72 of *E. coli* glutaredoxin, residues 1–7, 14–28, 31–37, 66–70, and 74–79 of T4 glutaredoxin, and residues 23–29, 32–46, 55–61, 76–80, and 88–93 of *E. coli* thioredoxin.

than each of these proteins resembles the *E. coli* thioredoxin, with r.m.s.d. values of 0.9 and 1.0 Å between the different glutaredoxins and of 1.3–1.6 Å relative to thioredoxin. Figure 6 shows the superposition of the oxidized forms of *E. coli* and T4 glutaredoxin using the backbone atoms of the above-listed 40 residues for the calculation of the superposition. For the two glutaredoxins, the alignment of residues based on the 3D structure extends to the last helix (residues 71–80 in *E. coli* glutaredoxin, residues 78–87 in T4 glutaredoxin), although this helix is shorter in the T4 protein. In the *E. coli* thioredoxin structures this C-terminal helix adopts a different orientation relative to the bulk of the molecule (Fig. 6). Insertions and/or deletions are apparent in particular for the polypeptide segments corresponding to the disordered regions 9–12 and 44–59 of *E. coli* glutaredoxin. (Note that *E. coli* thioredoxin contains an additional β-strand and an extra helix at the N-terminus that are not shown in Fig. 6.)

The orientation of the second helix relative to the core of the molecule is different in the three proteins, although this helix occupies about the same space with respect to the β-sheet. Due to the low precision with which the orientation of this helix is defined by the NMR data in both oxidation states of *E. coli* glutaredoxin (Fig. 1 and Sodano et al., 1991b), it is difficult to assess the relevance of this apparent structural difference.

Environment of the redox-active disulfide bond and functional implications

In an effort to explain the extraordinarily low pK_a value of Cys 11 (Björnberg & Holmgren, unpublished results), we have examined the 3D structure of reduced *E. coli* glutaredoxin for potential interactions with the thiol group of Cys 11. The only positively charged residue positioned in such a manner that it could interact with Cys 11 is Arg 8. Indeed, the positive charge at this position is conserved in all three mammalian glutaredoxins sequenced thus far (Hopper et al., 1989). Confirmation of the importance of Arg 8 may in the future be obtained from mutational studies, but its unique positioning in the molecular model is highly suggestive. In this context it is interesting that Nikkola et al. (1991) have, from modeling of glutathione into a cleft formed by residues 12–16 and 64–66 of T4 glutaredoxin, suggested that Arg 8 in *E. coli* glutaredoxin might play a role in the binding of glutathione.

As has been observed for *E. coli* thioredoxin and T4 glutaredoxin (Eklund et al., 1984), the redox-active dithiol region is accessible from the surface on one side of *E. coli* glutaredoxin, but is quite shielded on the other side, i.e., Cys 14 is buried and inaccessible, whereas Cys 11 is readily solvent accessible (Table 6). This helps to rationalize the high reactivity of Cys 11 and lack of reactivity of Cys 14 in alkylation studies of the reduced protein with iodoacetic acid (Björnberg & Holmgren, unpublished results). Inspection of the molecular structure shows that Gly 10, Val 15, Lys 18, and Tyr 35 significantly block approach to the side-chain thiol of Cys 14.

Interaction surface for protein–protein interactions with E. coli glutaredoxin

The side chain of Cys 11 is exposed on the surface-accessible side in the reduced protein. A hydrophobic surface on this accessible side in the homologous regions of T4 glutaredoxin and *E. coli* thioredoxin has previously been proposed to be the interaction surface for protein–protein interaction for these proteins, in particular with ribonucleotide reductase (Eklund et al., 1984). As for T4 glutaredoxin and *E. coli* thioredoxin, *E. coli* glutaredoxin also possesses an exposed surface in this region containing—apart from Cys 11—Arg 8, Pro 12, Tyr 13, Ile 38, Thr 58, Val 59, Pro 60, Gly 71, Tyr 72, and Thr 73 (Table 6), which includes a number of nonpolar residues (Fig. 7). The majority of these side chains are not among the well-defined core side chains (Table 3). Nonetheless, the relative positioning and general topology of this region can be discerned from Figure 7 and Kinemage 4. Among the residues in the presumed interfaces, Ile 38, Pro 60, and Gly 71 are conserved among T4 glutaredoxin, *E. coli* thioredoxin, and *E. coli* glutaredoxin. Tyr 13 and Thr 58 are conserved in *E. coli* and T4 glutaredoxin. In addition,

Table 6. *Comparison of the average solvent-accessible surface areas for residues involved in the active site and in the proposed interaction surfaces of reduced and oxidized E. coli glutaredoxin*

	Percentage accessible surface area (range)[a]	
Residue	⟨OX⟩	⟨RED⟩
Arg 8	32.2 (8.7...43.0)	38.1 (24.4...49.5)
Cys 11	12.6 (4.5...24.7)	27.4 (4.6...44.3)
Pro 12	48.7 (44.9...53.1)	44.7 (34.6...54.1)
Tyr 13	37.7 (28.0...49.6)	40.0 (26.4...53.5)
Cys 14	2.1 (0.1...7.4)	2.9 (0.5...7.8)
Ile 38	12.2 (3.6...19.2)	14.9 (8.6...22.2)
Thr 58	30.7 (7.7...46.6)	38.0 (12.6...46.7)
Val 59	24.6 (10.3...39.0)	24.6 (9.0...40.6)
Pro 60	4.6 (0.3...15.7)	8.3 (3.2...20.6)
Gly 71	8.0 (0.5...21.4)	11.5 (1.8...20.6)
Tyr 72	16.3 (10.1...23.4)	22.7 (10.4...31.7)
Thr 73	42.6 (32.7...50.3)	43.7 (37.7...47.3)

[a] ⟨OX⟩ and ⟨RED⟩ represent the 20 conformers of oxidized and reduced *E. coli* glutaredoxin that were used to characterize the solution conformation. Solvent-accessible surface areas were calculated with a modified version (Billeter et al., 1990) of the ANAREA program (Richmond, 1984). The values given are the averages of the values calculated for the individual 20 conformers (and the range of values).

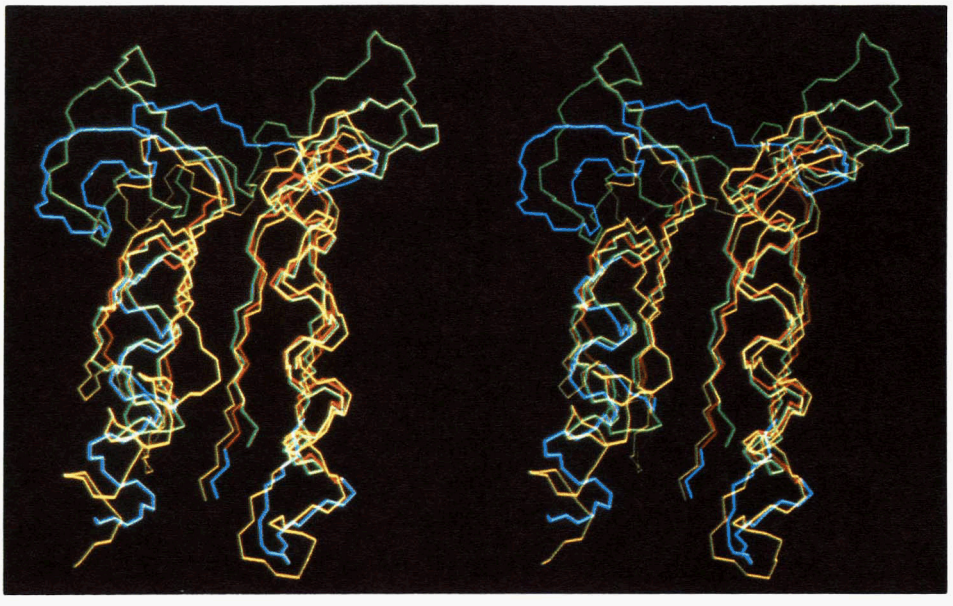

Fig. 6. Stereo view of a superposition of the averaged coordinates of the NMR solution structure of the oxidized form of *E. coli* glutaredoxin (blue and red lines), the X-ray crystal structure of oxidized T4 glutaredoxin (green line; Eklund et al., 1991), and the X-ray crystal structure of the oxidized form of *E. coli* thioredoxin (yellow line; Katti et al., 1990; for this structure the first 21 residues are not shown). Those residues of *E. coli* glutaredoxin used for the superposition are colored red. The viewing angle for the *E. coli* glutaredoxin structure is the same as in Figures 1 and 2. For the superposition the N, C^{α}, and C′ atoms of residues 2–8, 11–25, 33–39, 60–64, and 67–72 of *E. coli* glutaredoxin, residues 1–7, 14–28, 31–37, 66–70, and 74–79 of T4 glutaredoxin, and residues 23–29, 32–46, 55–61, 76–80, and 88–93 of *E. coli* thioredoxin were used.

Tyr 13, Thr 58, Val 59, Pro 60, Gly 71, and Thr 73 are identical in *E. coli* and calf thymus glutaredoxin, and Arg 8 is conservatively substituted by lysine in the known mammalian glutaredoxins (Hopper et al., 1989). (In this context it seems worthwhile to point out that arginines are quite commonly found at protein–protein interfaces [Janin et al., 1988].) The high degree of conservation suggests that this is the region of protein–protein interaction for *E. coli* glutaredoxin as well as the other proteins considered here.

Calculation of the accessible surface areas for the above residues proposed to play a role in the interaction surface (Table 6) yields several interesting results. The total accessible surface area of these residues is ca. 800 $Å^2$, well within the 600–1,000-$Å^2$ surface area observed to be buried in protein–protein recognition sites that have been structurally characterized thus far (Janin & Chothia, 1990). With the exception of Pro 12 and Val 59, the accessible surface area for all of these residues is larger in the reduced form of *E. coli* glutaredoxin. Although some of the changes are relatively small, the consistent trend to higher accessible surface area is quite suggestive. In particular, the accessible surface areas of Pro 60, Thr 58, and Tyr 72 increase significantly upon reduction (Table 6). Because, on the one hand, the reduced protein binds quite tightly to ribonucleotide reductase, with a K_m of 0.13 μM (Holmgren, 1979), but must on the other hand dissociate once it is oxidized, these data suggest an interesting mechanism for the dissociation of the protein upon oxidation on the basis of subtle differences in the 3D structures of the two oxidation states: In addition to the loss of the disulfide bond to ribonucleotide reductase, the diminished accessible surface area of the residues on the protein–protein interaction surface would reduce the binding affinity to the reductase and thereby promote dissociation.

Because *E. coli* glutaredoxin, T4 glutaredoxin, and *E. coli* thioredoxin differ in their interactions with other proteins (summarized in Eklund et al., 1984) and thioredoxin is a more promiscuous reductant than the other two proteins, it is instructive also to examine the differences among the three proteins in this proposed interaction region. Arg 8 in *E. coli* glutaredoxin is substituted by tyrosine in T4 glutaredoxin and by alanine in thioredoxin, which are pronouncedly nonconservative substitutions that may play a role in determining the different specificities of these proteins. Among the active-site residues, Pro 12 in *E. coli* glutaredoxin is substituted by Val in T4 glutaredoxin and by Gly in thioredoxin, whereas Tyr 13 is conserved in T4 glutaredoxin but substituted by Pro in thioredoxin (Fig. 5). Clearly, thioredoxin presents the least steric bulk in this region, with the Gly–Pro active-site sequence and Ala in position 29; this correlates well with its less specific reactivity. Thr 58 is conserved in *E.*

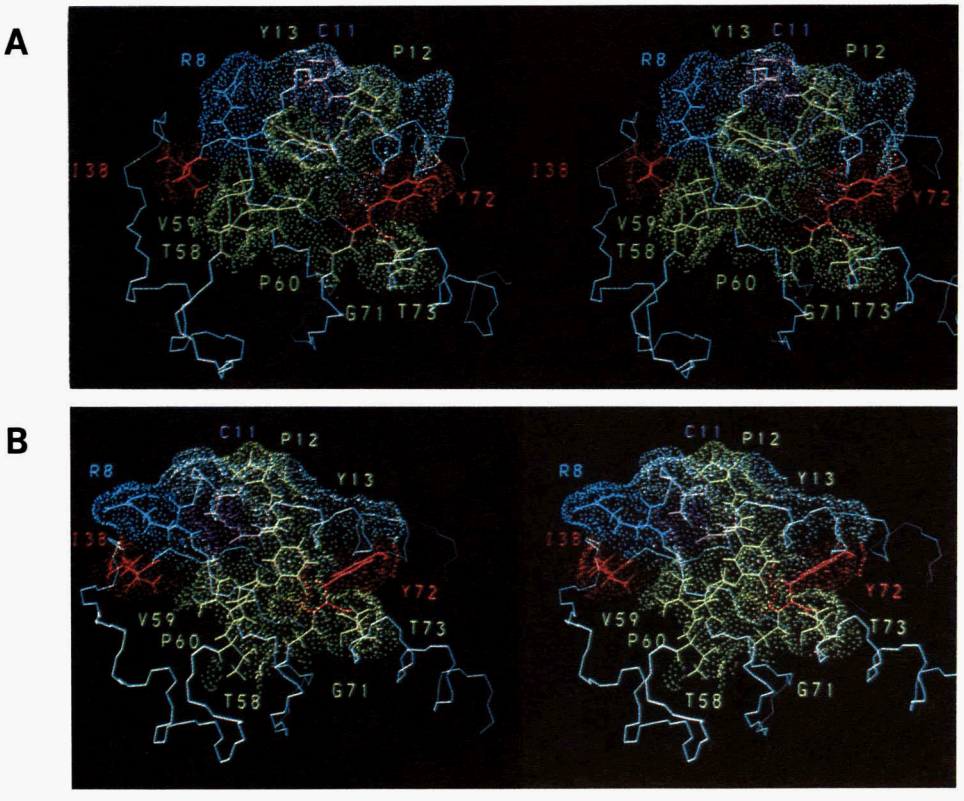

Fig. 7. Stereo views of the conformers of reduced **(A)** and oxidized **(B)** *E. coli* glutaredoxin, respectively, that have the smallest r.m.s.d. values relative to the mean coordinates for the corresponding solution conformation. The proposed interaction surface is shown, and the solvent-accessible surfaces are identified. The accessible surfaces were calculated with the program of Connolly (1983a,b), including the hydrogen atoms of the protein and using a probe of radius 1.4 Å. Residues mentioned in the text are colored as follows: Cys 11 and Cys 14, purple; Ile 38 and Tyr 72, which are the only residues in this area belonging to the well-defined core side chains (Table 3), red; the lone charged residue, Arg 8, blue; all others, i.e., Pro 12, Tyr 13, Thr 58, Val 59, Pro 60, Gly 71, and Thr 73, green.

coli and T4 glutaredoxin but is substituted by Gly in thioredoxin, which again presents less steric demands than in the glutaredoxins. Val 59 is substituted by Ile in thioredoxin and by Met in T4 glutaredoxin, which could be another source for the different affinities of *E. coli* glutaredoxin and T4 glutaredoxin for *E. coli* ribonucleotide reductase. Tyr 72 in *E. coli* glutaredoxin is substituted by Phe in T4 glutaredoxin and by Ala in thioredoxin, once more adding to a sterically less demanding surface for thioredoxin when compared with the glutaredoxins. Thr 73 is substituted by Leu in thioredoxin and by Asp in T4 glutaredoxin, which may further add to the differing specificities. In addition to the above, the loop preceding the active site in T4 glutaredoxin is extended relative to that in *E. coli* glutaredoxin and occupies space not occupied by *E. coli* glutaredoxin. This loop could play a role in preventing the interaction of T4 glutaredoxin with *E. coli* ribonucleotide reductase and thus provide for differences in specificity. Clearly, a number of interesting sites have been identified as potentially important for the interactions of these three proteins with other proteins, and these structural data could well serve as a basis for mutagenesis studies of all three proteins in attempts to further substantiate the present, still largely hypothetical notions about function and specificity.

Methods

NMR measurements

NMR spectroscopy was used as described previously (Sodano et al., 1991a). For the collection of upper bounds on ^1H–^1H distances, 2D nuclear Overhauser enhancement spectroscopy (NOESY) spectra (Anil-Kumar et al., 1980) with a mixing time of 40 ms were recorded in both H_2O and D_2O. Spin–spin coupling constants $^3J_{HN\alpha}$ were measured using the method of Neri et al. (1990). The spin–spin coupling constants $^3J_{\alpha\beta}$ were measured in an exclusive COSY spectrum (Griesinger et al., 1985) recorded in D_2O solution. Additionally, a 3D ^{15}N-correlated [^1H,^1H]-NOESY spectrum of the ^{15}N-labeled protein was recorded using the experimental scheme of Messerle et al. (1989) and employed to resolve ambiguities in the 2D [^1H,^1H]-NOESY spectra.

Structure calculations and structure comparisons

The calculation of the structure of the oxidized form of *E. coli* glutaredoxin from the NMR data (Wüthrich, 1986, 1989) followed the procedure used for the reduced form, which was described in detail by Sodano et al. (1991b). In short, the data analysis started with the program HABAS (Güntert et al., 1989) to make an initial check on the NMR data, to convert coupling constants into dihedral angle constraints, and to obtain stereospecific assignments for pairs of diastereotopic substituents. Next, distance geometry calculations with the program DIANA (Güntert et al., 1991a) yielded a set of folded glutaredoxin structures, which were used to unambiguously assign additional cross peaks in the NOESY spectra and to obtain additional stereospecific assignments with the program GLOMSA (Güntert et al., 1991b), e.g., for the valine and leucine methyl groups. The more complete set of input data thus obtained were used for a second round of DIANA calculations, and the resulting conformers were treated with a simulated annealing procedure using the program X-PLOR (Brünger, 1990). A set of 20 final conformers thus obtained describes the 3D fold of oxidized *E. coli* glutaredoxin in solution as well as the structural variability observed for different parts of the protein.

For the evaluation of the structure of *E. coli* glutaredoxin and for the comparison with other structures, r.m.s.d. values were calculated for selected sets of atoms. The r.m.s.d. values describe the spatial coincidence of the selected atoms when each atom contributes with equal weight to the spatial superposition. Structural variability was further evaluated by superposing the well-defined parts of the protein, followed by calculation of the displacements in atomic positions for other segments of the polypeptide chain (Billeter et al., 1989).

Determination of amide proton exchange rates

Two factors imposed some limitations on the selection of optimal conditions for amide proton exchange studies (Wüthrich, 1986). Because glutaredoxin starts to aggregate at pH values below 7.0 and reduced glutaredoxin begins to denature at pH 6.0, exchange experiments with both forms of the protein were carried out at pH 6.5. Furthermore, because we observed significant line broadening at 10 °C, particularly for oxidized glutaredoxin, the exchange measurements were recorded at 20 °C. Slowed exchange of amide protons was identified in the following manner. A sample of lyophilized ^{15}N-labeled glutaredoxin was dissolved at 4 °C in 50 mM potassium phosphate, pH 6.5, in D_2O (plus 4 equivalents of DTT for the reduced sample) to a final concentration of 1.5 mM. The sample was purged with argon for 2 min, then inserted into the preshimmed spectrometer, and data acquisition was started within 15 min after dissolving the protein. A series of 26 heteronuclear [^{15}N,^{1}H]-COSY spectra (Bodenhausen & Ruben, 1980) with 128 t_1 increments and 8 scans per t_1 value (t_{1max} = 20 ms, t_{2max} = 170 ms) for a measuring time of 25 min per spectrum was recorded over 11 h. The spectra were processed with $\pi/4$- and $\pi/3$-shifted sine bell apodization in ω_2 and ω_1, respectively, and baseline-corrected in ω_2. Those amide protons that were detectable in the first spectrum were deemed to have slowed exchange.

For quantification of the rates of exchange, pairs of COSY spectra were added together to improve the signal-to-noise ratio, and well-separated cross peaks were integrated in each of the spectra. The data were fitted to a single exponential, assuming pseudo-first-order kinetics to obtain the rate constants for exchange.

Acknowledgments

We thank Dr. K.V.R. Chary for help with the recording of the NMR spectra, and R. Marani for the careful processing of the manuscript. We also thank Dr. P. Wright for providing coordinates of the NMR solution structure of reduced *E. coli* thioredoxin and Dr. H. Eklund for providing coordinates of the X-ray crystal structures of oxidized *E. coli* thioredoxin and T4 glutaredoxin. Financial support was obtained from the Schweizerischer Nationalfonds (project 31.25174.88), EMBO (long-term postdoctoral fellowship to P.S.), the Swedish Cancer Society (961), the Karolinska Institute, and the US National Institutes of Health (postdoctoral fellowship to J.H.B.).

References

Anil-Kumar, Ernst, R.R., & Wüthrich, K. (1980). A two-dimensional nuclear Overhauser enhancement (2D NOE) experiment for the elucidation of complete proton-proton cross-relaxation networks in biological macromolecules. *Biochem. Biophys. Res. Commun. 95*, 1-6.

Billeter, M., Kline, A.D., Braum, W., Huber, R., & Wüthrich, K. (1989). Comparison of the high-resolution structures of the α-amylase inhibitor tendamistat determined by nuclear magnetic resonance in solution and by X-ray diffraction in single crystals. *J. Mol. Biol. 206*, 677-687.

Billeter, M., Qian, Y.Q., Otting, G., Müller, M., Gehring, W.J., & Wüthrich, K. (1990). Determination of the three-dimensional structure of the *antennapedia* homeodomain from *Drosophila* in solution by ^{1}H nuclear magnetic resonance spectroscopy. *J. Mol. Biol. 214*, 183-197.

Bodenhausen, G. & Ruben, D. (1980). Natural abundance nitrogen-15 NMR by enhanced heteronuclear spectroscopy. *Chem. Phys. Lett. 69*, 185.

Brünger, A.T. (1990). *X-PLOR, Version 2.1, User Manual.* Yale University, New Haven, Connecticut.

Connolly, M.L. (1983a). Solvent-accessible surfaces of proteins and nucleic acids. *Science 221*, 709-713.

Connolly, M.L. (1983b). Analytical molecular surface calculation. *J. Appl. Crystallogr. 16*, 548-558.

Dyson, H.J., Gippert, G.P., Case, D.A., Holmgren, A., & Wright, P.E. (1990). Three-dimensional solution structure of the reduced form of *E. coli* thioredoxin determined by nuclear magnetic resonance spectroscopy. *Biochemistry 29*, 4129-4136.

Eklund, H., Cambillau, C., Sjöberg, B.M., Holmgren, A., Jörnvall, H., Höög, J.O., & Brändén, C.I. (1984). Conformational and functional similarities between glutaredoxin and thioredoxins. *EMBO J. 3*, 1443-1449.

Eklund, H., Ingelman, M., Söderberg, B.O., Uhlin, T., Nordlund, P.,

Nikkola, M., & Joelsson, T. (1992). The structure of oxidized bacteriophage T4 glutaredoxin (thioredoxin). *J. Mol. Biol.* (submitted).
Griesinger, C., Sorensen, O.W., & Ernst, R.R. (1985). Two-dimensional correlation of connected NMR transitions. *J. Am. Chem. Soc. 107*, 6394-6396.
Güntert, P., Braun, W., Billeter, M., & Wüthrich, K. (1989). Automated stereospecific ^{1}H NMR assignments and their impact on the precision of protein structure determinations in solution. *J. Am. Chem. Soc. 111*, 3997-4004.
Güntert, P., Braun, W., & Wüthrich, K. (1991a). Efficient computation of three-dimensional protein structures in solution from nuclear magnetic resonance data using the program DIANA and the supporting programs CALIBA, HABAS and GLOMSA. *J. Mol. Biol. 217*, 517-530.
Güntert, P., Qian, Y.Q., Otting, G., Müller, M., Gehring, W.J., & Wüthrich, K. (1991b). Structure determination of the *Antp(C39→S)* homeodomain from nuclear magnetic resonance data in solution using a novel strategy for the structure calculation with the programs DIANA, CALIBA, HABAS and GLOMSA. *J. Mol. Biol. 217*, 531-540.
Holmgren, A. (1979). Glutathione-dependent synthesis of deoxyribonucleotides. *J. Biol. Chem. 254*, 3672-3678.
Holmgren, A. (1985). Thioredoxin. *Annu. Rev. Biochem. 54*, 237-271.
Holmgren, A. (1989). Thioredoxin and glutaredoxin systems. *J. Biol. Chem. 264*, 13963-13966.
Holmgren, A., Söderberg, B.-O., Eklund, H., & Brändén, C.-I. (1975). Three-dimensional structure of *Escherichia coli* thioredoxin-S_2 to 2.8 Å resolution. *Proc. Natl. Acad. Sci. USA 72*(6), 2305-2309.
Höög, J.-O., Jörnvall, H., Holmgren, A., Carlquist, M., & Persson, M. (1983). The primary structure of *E. coli* glutaredoxin. *Eur. J. Biochem. 136*, 223-232.
Hopper, S., Johnson, R.S., Vath, J.E., & Biemann, K. (1989). Glutaredoxin from rabbit bone marrow. *J. Biol. Chem. 264*, 20438-20447.
Janin, J. & Chothia, C. (1990). The structure of protein-protein recognition sites. *J. Biol. Chem. 265*, 16027-16030.
Janin, J., Miller, S., & Chothia, C. (1988). Surface, subunit interfaces and interior of oligomeric proteins. *J. Mol. Biol. 204*, 155-164.
Katti, S.K., LeMaster, D.M., & Eklund, H. (1990). Crystal structure of thioredoxin from *E. coli* at 1.68 Å resolution. *J. Mol. Biol. 212*, 167-184.
Messerle, B., Wider, G., Otting, G., Weber, C., & Wüthrich, K. (1989). Solvent suppression using a spin lock in 2D and 3D NMR spectroscopy with H_2O solutions. *J. Magn. Reson. 85*, 608-613.
Nikkola, M., Gleason, F.K., Saarinen, M., Joelsson, T., Björnberg, O., & Eklund, H. (1991). A putative glutathione-binding site in T4 glutaredoxin investigated by site-directed mutagenesis. *J. Biol. Chem. 266*, 16105-16112.
Neri, D., Otting, G., & Wüthrich, K. (1990). New nuclear magnetic resonance experiment for measurements of the vicinal coupling constants $^3J_{HN\alpha}$ in proteins. *J. Am. Chem. Soc. 112*, 3663-3665.
Richmond, T.J. (1984). Solvent accessible surface area and excluded volume in proteins. *J. Mol. Biol. 178*, 63-89.
Sodano, P., Chary, K.V.R., Björnberg, O., Holmgren, A., Kren, B., Fuchs, J.A., & Wüthrich, K. (1991a). Nuclear magnetic resonance studies of recombinant *E. coli* glutaredoxin. Sequence-specific assignments and secondary structure determination for the oxidized form. *Eur. J. Biochem. 200*, 369-377.
Sodano, P., Xia, T.-H., Bushweller, J.H., Björnberg, O., Holmgren, A., Billeter, M., & Wüthrich, K. (1991b). Sequence-specific ^{1}H NMR assignments and determination of the three-dimensional structure of reduced *E. coli* glutaredoxin. *J. Mol. Biol. 221*, 1311-1324.
Söderberg, B.-O., Sjöberg, B.-M., Sonnerstam, U., & Brändén, C.-I. (1978). Three-dimensional structure of thioredoxin induced by bacteriophage T4. *Proc. Natl. Acad. Sci. USA 75*, 5827-5830.
Wüthrich, K. (1986). *NMR of Proteins and Nucleic Acids.* Wiley, New York.
Wüthrich, K. (1989). Protein structure determination in solution by nuclear magnetic resonance spectroscopy. *Science 243*, 45-50.